COMMUNICATIONS IN SCIENCE AND TECHNOLOGY
Homepage: cst.kipmi.or.id

Separation of heavy metal pollutants by micellar-enhanced ultrafiltration membrane system and its surfactant recovery

Nita Aryanti*, Heru Susanto, I Nyoman Widiasa, Nur Rokhati, Aininu Nafiunisa, Alifia Rizki Adina, Arnaldi Dwilaksita

Department of Chemical Engineering, Diponegoro University, Semarang 50275, Indonesia

Article history:
Received: 13 January 2026 / Received in revised form: 21 May 2026 / Accepted: 30 May 2026

Abstract

Micellar-enhanced ultrafiltration (MEUF) is an effective treatment for treating heavy metal effluents. However, excessive use of synthetic surfactants leads to more serious problems, thereby highlighting the significance of surfactant recovery. This present study focuses on the recovery of surfactants while preserving their capacity to entrap metal ions. In this study, the acidification method was utilized to dissociate metal ions (Cu^{2+} and Cd^{2+}) from the surfactant micelles. The findings demonstrate that the lowest critical micelle concentration found at pH 1, with 91% and 87% of the surfactant recovered for Cu^{2+} and Cd^{2+} system, respectively. The spontaneous occurrence of acidic surfactant micellization was thermodynamically validated, as evidenced by negative ΔG_m values. Furthermore, the recovered surfactant exhibits high level of rejection and indicates an intermediate-blocking mechanism (R^2>0.99). The findings highlight acid-assisted MEUF as a scalable approach for efficient metal removal and surfactant recovery, in turn, reducing chemical consumption and environmental impact.

Keywords: Ultrafiltration; fouling; heavy metals; critical micelle concentration

1. Introduction

The presence of heavy metal contaminants in wastewater has long been a serious environmental concern, posing a significant threat to the health of living organisms and ecosystems, even at very low concentrations [1]. Despite the effectiveness of wastewater treatment facilities, the discharge of heavy metal pollutants into water systems was hindered [2]. The treatment of heavy-metal wastewater has been discussed in a previous study, which employed several methods, including ion exchange [3], adsorption [4,5], precipitation [6], and reverse osmosis [7]. Of various technologies available, membrane ultrafiltration offers several advantages, including low energy consumption, simple equipment and environmental sustainability [8,9].

The integration methods of ultrafiltration with surfactants are known as micellar enhanced ultrafiltration (MEUF), which has been demonstrated to be effective in the separation of contaminants, including heavy metal ions, such as Cd^{2+}, Co^{2+}, Ni^{2+}, Mn^{2+}, Zn^{2+} and Cu^{2+} [1,10,11]. The utilization of MEUF in the treatment of wastewater has been demonstrated to yield high separation efficiency with low energy consumption and simple equipment [12]. MEUF works by utilizing the surfactant micelle-forming properties at a concentration above the critical micelle concentration (CMC), a structure with a hydrophobic center and a hydrophilic exterior [13]. Due to these properties, heavy metal ions tend to be trapped within the micelle structure, thereby forming larger molecule complexes [14]. The aggregate of surfactant micelles with entrapped metal ions inside of it is larger than the pores of the ultrafiltration membrane, and thus unable to pass through it [15]. It subsequently allows the separation of both metal-bound micelles and the surfactant micelles. The most widely employed surfactant in the MEUF process is sodium dodecyl sulfate (SDS), an anionic surfactant that has been recognized for its efficacy in removing heavy metal ions through the MEUF process.

However, a further issue arises when the retentate from the ultrafiltration process is left untreated due to the high concentration of heavy metal content and uneconomically wasted surfactant. Excessive surfactant concentrations above the CMC can result in secondary pollution, necessitating the recovery of surfactants [12]. Moreover, the reuse of surfactants recovered from the retentate system has been demonstrated to be profitable and complete separation of heavy metal is critical [16]. Various surfactant recovery techniques have been developed, including foam fractionation [17], acidification [18], flooding of alkali-surfactant [19], coagulation, advance

* Corresponding author.
Email: nita.aryanti@che.undip.ac.id
https://doi.org/10.21924/cst.11.1.2026.1887

oxidation and adsorption [20,21]. In the realm of the recovery methodologies, acidification offers simpler and efficient process to recover surfactants. This process involves the separation of entrapped heavy metal ions from the surfactant micelles by means of the interruption of the bond between metal ions and surfactant, facilitated by the presence of H^+ ions [22]. This process allows micelles to be retained, while metal ions pass through the ultrafiltration membrane based on size exclusion [23]. However, the majority of previous studies treat surfactants as pollutants to be removed, with limited evaluation of the subsequent reuse of recovered surfactants in further separation cycles.

Despite the previous efforts, there is still a lack of understanding of the MEUF process for removing heavy metals under the influence of pH. Moreover, there is a paucity of comprehensive study on the effect of pH on the micellization thermodynamics, critical micelle concentration and surfactant recovery efficiency was understudied despite the pH dependency of the effluent in real-world process. In particular, the integration of acidification with ultrafiltration for simultaneous extraction of metal ions from the surfactant micelles and recovery and reuse of the surfactant is an area which has received little attention from researchers. Consequently, the present study aims to address this gap by investigating surfactant recovery using acidification-integrated ultrafiltration. This study evaluated the thermodynamic feasibility of micelle formation at various pH conditions. In addition, the effect of surfactant concentration on surfactant recovery and performance analysis on the recovered surfactant were conducted in this study.

2. Materials and Methods

2.1. Materials

In this study, the materials employed consist of the surfactant Sodium Dodecyl Sulfate (SDS) (99.9%, Merck), in conjunction with the metal ions of $Cu(NO_3)_2$ (99.9%, Merck) and $Cd(NO_3)_2.4H_2O$ (98%, Merck). These substances were utilized to produce models of heavy metal wastewater. Sulfuric acid was utilized for acidification, while a polyether sulfone (PES) flat-sheet membrane with a molecular weight cutoff of 1 kDa was employed in the MEUF process.

2.2. Preparation of wastewater model solution and acidification

A model of heavy metal wastewater was employed as the feed for the ultrafiltration process. The model solution was prepared by means of the dissolution of 100 mg of $Cu(NO_3)_2$ or $Cd(NO_3)_2.4H_2O$. The surfactant concentration utilized in this study was 2.02 g of SDS in 1000 ml distilled water, which was slightly higher than the CMC at room temperature. This concentration is pivotal to ensure the completion of micelle formation, which is required for efficient entrapment of heavy metals during the MEUF process. The solution was subjected to stirring for a duration of 1 hour at a temperature of approximately 25°C at a stirring speed of 100 rpm.

Acidification was subsequently carried out through the addition of sulfuric acid to the wastewater model solution to adjust the pH (1, 2, 3) selected in accordance to the preliminary experiments [24]. The mixture was then subjected to an additional hour of stirring at a speed of 100 rpm at a temperature of approximately 25°C. In such conditions, efficient dissociation of the metal ions was guaranteed while maintaining micelle integrity [24]. These selected conditions represent a practical range for the laboratory and industrial works, where the adjustment of pH can be simply applied during the heavy metal desorption.

2.3. Conductivity analysis

Conductivity analysis was conducted for two primary objectives: firstly to determine the CMC value of the surfactant and secondly to assess the effect of pH adjustment on the solution. In this study, the CMC value was determined using the electrical conductivity measurement method with a conductivity meter from AZ Instrument, Taiwan. Conductivity was measured by continuous addition of surfactant concentrations to the solution at a specific pH. The CMC value was identified through the breakpoint on the curve relating conductivity to surfactant concentration [25].

2.4. Thermodynamic analysis of micellization

Thermodynamic parameters are of crucial role in understanding the micellization process of surfactants, for instance the standard Gibbs free energy of micellization ($\Delta G°_m$). The value of $\Delta G°_m$ can be utilized as a parameter to determine the tendency of surfactants to form micelles. The $\Delta G°_m$ value of SDS surfactant, in the presence of metal ions and the influence of solution pH, is evaluated using Eq. (1).

$$\Delta G_m^o = (2 - \alpha)RT \ln X_{cmc} \quad (1)$$

where X_cmc represents the mole fraction of the surfactant at CMC, and R is the ideal gas constant (8.314 J/K·mol). Meanwhile, α represents the degree of micellization ionization, with the value of α obtained through Eq. (2) [17].

$$\alpha = \frac{S_2}{S_1} \quad (2)$$

where S_2 represents the premicellar slope, while S_1 represents the postmicellar slope on the curve obtained from the surface tension analysis [26].

2.5. Ultrafiltration pretreatment

The solution obtained from acidification was utilized as feed in the ultrafiltration process. The ultrafiltration process was conducted at room temperature using the membrane crossflow filtration. During the filtration process, the flow rate remained unchanged, with a consistent pressure of 2.5 bar. The ultrafiltration process scheme is illustrated in Fig. 1. The membrane utilized in the ultrafiltration process was polyether sulfone (PES) with a molecular weight cutoff of 1 kDa. The ultrafiltration process was continued until reaching a permeate-to-retentate solution ratio of 60:40. Subsequently, the retentate is subjected to further process.

2.6. Ultrafiltration of the heavy metal assisted by surfactant micelles

In this stage, the Micellar Enhanced Ultrafiltration (MEUF) process involved the reuse of the surfactant recovered from the ultrafiltration process to bind metal ions. The retentate solution from the previous ultrafiltration process was subsequently mixed with $Cu(NO_3)_2$ or $Cd(NO_3)_2{\cdot}4H_2O$. The solution was stirred for 1 hour at a speed of 100 rpm at room temperature (25°C) to ensure the solution homogeneity and complete entrapment of metal ions into the surfactant micelles. Subsequently, the MEUF process was conducted using the same membrane crossflow filtration instrument employed in the ultrafiltration process at a room temperature and fixed pressure of 2.5 bar. Furthermore, PES membrane (1 kDa) was utilized in the MEUF process, undergoing a one-hour distillation water compacting procedure prior to each filtration batch. Eventually, the permeate solution obtained from the MEUF process was analyzed using atomic absorption spectroscopy to determine the concentration of metal ions in the permeate solution that passed through the membrane without being bound to the recovered surfactant micelles. Fig. 1 depicts the schematic diagram of the MEUF process to recover the surfactant.

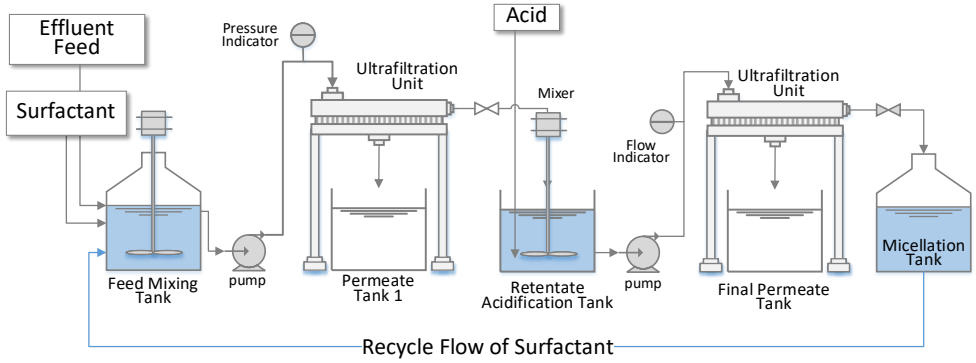

Fig. 1. Schematic diagram of the overall process of surfactant recovery and MEUF using the recovered surfactant

2.7. Analysis of surfactant recovery and metal ion rejection

The concentration of the anionic surfactant sodium dodecyl sulfate (SDS) was determined after the separation of the metal ion by acidification by means of UV-Vis spectrophotometry, a standard method for measuring surfactant content in a solution sample, as explained in the previous study [27]. The analysis was based on the formation of a yellow-colored complex of samples containing SDS with acridine orange dyes. Initially, the sample was diluted with water to yield a solution of 2 mg/L solution. It was then mixed with the dye indicator, extracted into toluene, and measured at 467 nm wavelength. Subsequently, the percentage rejection of SDS was calculated using Eq. (3) [28].

$$R_0(\%) = \frac{C_S V_S}{C_i V_i} \times 100\% \quad (3)$$

where C_s is the surfactant concentration in the retentate solution, and C_i is the surfactant concentration in the feed solution, while V_s is the retentate volume and V_i is the initial volume of the feed solution.

Furthermore, the metal ions left inside the core of the micelles can be neglected due to their sequestered structure and minuscule amount, which is less likely to interfere with the spectrophotometry analysis. Meanwhile, the concentration of the metal ions in the retentate was determined using atomic absorption spectroscopy (AAS). The efficiency of metal ion separation from the surfactant was calculated using Eq. 4.

$$R_0(\%) = \frac{C_P V_P}{C_f V_i} \times 100\% \quad (4)$$

where R represents the efficiency of metal ion separation (Cu or Cd) from the surfactant, C_P is the concentration of metal ions in the permeate solution, and C_f is the concentration of metal ions in the feed solution, while V_P represents the volume of the permeate and V_i represents the volume of the feed solution.

2.8. Analysis of flux and model of membrane fouling

Membrane flux analysis was conducted to determine the effect of varying solution pH on membrane flux activity. The analysis involved the measurement of the volume of the retentate solution at 10-minute intervals, with subsequent calculation of the mean value using the following equation [29].

$$J = \frac{volume}{t \times A} \quad (5)$$

where t represents time and A is the surface area of the membrane used.

Membrane fouling analysis was performed using the Hermia model, which consists of four Hermia models that describe the fouling conditions on the membrane [30,31]. These equations include complete pore blocking, internal pore blocking, intermediate pore blocking, and cake formation. These were calculated based on the initial Eq. (6).

$$\frac{d^2t}{dV^2} = k\left(\frac{dt}{dV}\right)^n \quad (6)$$

Complete pore blocking (model 1) indicates the deposition of pollutants in particle form on the overall surface of the membrane, with the result that the surface of the membrane pores is completely filled. The n value for this fouling was 2, and the derived equation is Eq. 7.

$$J = J_0 \times exp(-K_c \times t) \quad (7)$$

The process of internal pore blocking, also referred to standard blocking (model 2) involves the blocking of pollutant particles within the internal space of the membrane pores. This results in a reduction in the size of the pores. The n value for this fouling was 1.5, and the derived equation is Eq. 8.

$$J = (J_0^{-0.5} + K_s \times t)^{-2} \quad (8)$$

The intermediate pore-blocking (model 3) mechanism occurred when deposited particles on the membrane pores, resulting in the formation of a layered structure that overlapped with one another on the membrane surface. The n value for this fouling was 1, and the derived equation was Eq. 9.

$$J = (J_0^{-1} + K_i \times t)^{-1} \quad (9)$$

Cake formation (model 4) was identified as the fouling mechanism where the pollutants completely clog the membrane surface and interact with each other, resulting in a multilayer of pollutant aggregate (cake). The n value for this fouling was determined to be 0.5 and derived into Eq. 10.

$$J = \left(J_0^{-2} + K_{cf} \times t\right)^{-0.5} \quad (10)$$

3. Results and Discussion

3.1. Effect of pH on the surfactant micelles

As demonstrated in Fig. 2, the pH of the solution has a significant influence on the critical micelle concentration (CMC) of anionic surfactants in the presence of sulfuric acid. A curve comprising two linear segments demonstrates different slopes when conductivity is measured as a function of surfactant concentration. The former line indicates the concentrations of surfactants below their CMCs, where surfactant monomers are present in solution. At higher surfactant concentrations, a second line with a different slope is drawn, owing to a change in conductivity; the intersection of the two lines indicates the measured CMC [32]. The mobility of ions in solution is of a crucial role. The addition of a surfactant to a solution results in an increase in the ion concentration, thereby enhancing the conductivity of the solution. This phenomenon is attributed to the electrostatic interactions between the oppositely charged surfactant and other ions [17].

Surfactant micellization represents a balance between hydrophobic interactions and electrostatic repulsion among the anionic headgroups. It has been demonstrated that the solutions exhibiting a lower pH value demonstrate higher conductivity values in view of the increase in the H^+ ions concentration in the solution. The increase in the presence of H^+ ion has been shown to result in an increase in electrostatic values, thus reducing the repulsive forces between the anionic surfactant headgroups. This, in turn, induces aggregation, micelle formation, and decreases the CMC [33]. Consequently, solutions with lower pH have higher electrostatic conductivity, and the CMC value is lower compared to the CMC of pure surfactants [34].

The CMC of SDS in pure water (pH 7) was previously reported at approximately 8.1–8.2 mM at 25 °C [26]. In this study, the CMC of SDS surfactant at pH 1, 2, and 3 were decreased to 3, 4, and 6 mM, respectively. It is demonstrated that the pH value has a direct impact on the CMC of pure anionic surfactants, thereby confirming the fundamental behavior of surfactants. In the presence of elevated H+ concentration (acidic condition), there was an increase in ionic strength and a decrease in electrostatic repulsion. This phenomenon facilitated micellization even at lower SDS concentration. As demonstrated in earlier study, a similar result showing a reduction in CMC has also been observed. This decline can be attributed to the presence of metal ions [35] and pH conditions [34], which have been shown to decrease the CMC of SDS surfactant. These results indicate that micelle formation is easier, which subsequently facilitates the separation of the surfactant from the solution [36]. The literatures confirms that ionic conditions have a significant effect on the CMC of ionic surfactant, in coherence with the results presented in this study.

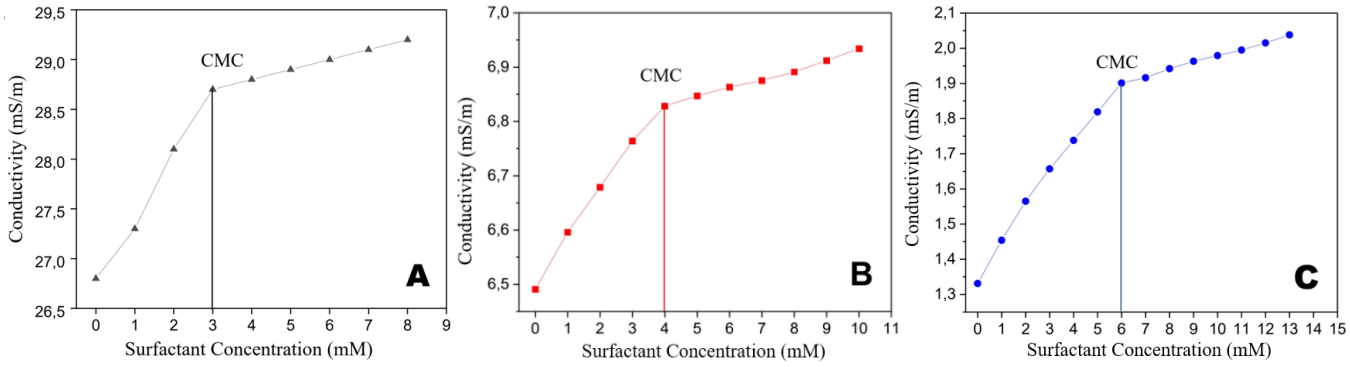

Fig. 2. Conductivity of surfactants in pH 1 (a), 2 (b), and 3 (c)

3.2. Standard value of Gibbs free energy of micellization

The micellization process is typically exothermic and spontaneous. Consequently, the value of the Gibbs free energy can indicate the favorable condition for micelle formation [37]. As depicted in Table 1, the thermodynamic parameters of the acidification process demonstrate a decline in the value of α with a decrease in pH. The decrease in α is attributable to the electrostatic interactions between the surfactant and H^+ ions resulting from the acidification process [17]. This phenomenon results in the bulk phase becoming enriched in H^+ ions and becoming more polar, thereby reducing the repulsive forces

between ions in the surfactant headgroups, thus enabling a greater number of ions with opposite charges to attach to the surface of the micelles [38]. Protonation of the surfactant headgroups has been demonstrated to reduce electrostatic repulsion, thereby facilitating tight molecular packing and enhanced micelle formation. As the headgroups become more closely spaced, ion pairing at the Stern layer of the micelles is promoted, allowing oppositely charged ions to bind more strongly to the micellar surface [39]. The present study aims to explore the effect of solution pH on the micellization process of anionic surfactants. This investigation will be achieved through the calculation of the standard Gibbs free energy of micellization.

Table 1. ΔG_m value in pH variations

pH	CMC (mM)	ΔG_m (kJ/mol)	α
1	3	-44.95	0.15
2	4	-42.50	0.20
3	6	-40.56	0.21

As illustrated in Table 1, a decrease in the pH of the solution is accompanied by an increase on the negative standard Gibbs free energy of micellization ($\Delta G°_m$ic). At the lowest pH level (pH 1), the standard Gibbs free energy of micellization is -44.95 kJ/mol, which is lower than the values obtained at other pH levels. The negative value on the calculated Gibbs free energy of micellization indicates that the formation of the micelle is a spontaneous process [37]. This observation aligns with previous findings that the CMC at pH 1 is lower in comparison to higher pH values. In comparison to the prior studies, the present study employs acidification in conjunction with UF, thereby enabling simultaneous micelle formation, metal ion removal, and surfactant recovery. The changes in the standard Gibbs free energy of micellization across different pH levels are attributed to alterations in the molecular structure of the monomers. Prior to the occurrence of micellization process, the monomers exhibit free movement freely within the solution. The addition of acid has been demonstrated to decrease the pH of the solution thereby increasing the concentration of H^+ ions at lower pH levels. This, in turn, restricts the movement of the monomers. The process of micelle formation is promoted by a reduction in the electrostatic repulsive forces among the negatively charged anionic surfactant headgroups [40].

3.3. Size of the micelles

The size of surfactant micelles can be determined by several factors, including surfactant concentration, temperature, pH, and electrolytes. In this investigation, dynamic light scattering (DLS) measurements are employed to determine the average size and size distribution of the produced surfactant micelles. The cumulant intensity and the average diameter are referred to as Z-average, which is calculated from the first cumulant [41]. For ionic surfactants, the pH of the solution and the concentration of surfactant are critical factors that affect the size of the surfactant micelles. For that reason, the observations are conducted at various pH values.

The results of the micelle size measurements are presented in Table 2. Conversely, as the pH of the solution decreases, the size of the resulting surfactant micelles increases. The Z-average of 6994.3 nm was measured at pH 1, and it was found to be higher than the values obtained at the other pH conditions. This result is significantly larger than the typical size of SDS micelles. The polydispersity index (PI) was found to be 3.141. Meanwhile, the mean micelle size at pH 2 and 3 are 1671.2 nm and 1595.6 nm, respectively. At a highly acidic pH, the negative charges on the head groups of SDS are significantly reduced, resulting in which leads to the aggregation of multiple micelles into larger clusters, a finding also found in the previous study [42–44]. In condition of extreme condition such as highly low pH, such aggregates may grow even bigger in size, resulting in the formation of non-micellar structures including bilayers or rod-like shapes, thereby resulting in higher measurement of Z-average [45].

Furthermore, the high polydispersity index (PI) has been demonstrated to facilitate the agglomeration of the micelles into substantial heterogeneous aggregates. The Polydispersity Index (PI) is a measure of the heterogeneity of a sample based on size. The PI value is derived from the size distribution within a sample, including agglomeration or aggregation during the analysis obtained through DLS. The presence of PI value greater than 1 indicates a broader particle size distribution, or alternatively, of polydisperse [46]. This finding demonstrates that pH has a significant influence on the size of the surfactant micelles produced. At low pH, the electrostatic repulsive forces between the negatively charged ionic surfactant headgroups decrease, facilitating the aggregation of surfactant monomers and the formation of more compact structures [40]. Moreover, surfactant micelles tend to show enhanced stability at low pH, thereby ensuring consistency during the analysis and process, resulting in a higher Z-average.

Table 2. Particle size of micelle in surfactant

pH	Z-Average (nm)	PI
1	6994.3	3.14
2	1671.2	1.75
3	1595.6	2.74

3.4. Evaluation of surfactant recovery

As depicted in Fig. 3, a decrease in pH is associated with an increase in surfactant recovery. Specifically, recovery at pH 1 ranges from approximately 74% to 91% when SDS concentration increases from 4 mM to 7 mM. At a pH of 2, the recovery ranges from approximately 63% to 81%, and at a pH of 3, it ranges from approximately 49% to 65%. At lower pH levels, an increase proportion of H^+ ions undergoes protonation of the SDS headgroups, thereby increasing ionic strength and reducing the electrostatic repulsion [39]. This process facilitates micelle aggregation and increases the available H^+ ions to detach the metal ions from the surfactant micelles. Consequently, the trend in the results can be explained mechanistically by the replacement of the metal ions on the surfactant micelles with the H^+ ions from the acid.

The results of the particle size analysis presented in Table 2 demonstrate that lower pH stimulates the formation of larger

surfactant micelles. This lower surface charge density is in relation to the aggregation of many surfactants in one micelle, thus promoting the displacement of multivalent metal ions during the recovery process [47]. This finding explains why surfactant recovery at 4 mM is higher at pH 1 compared to pH 3, even at the same SDS concentration, as demonstrated in Fig. 3(a) and 3(b). Meanwhile, at a concentration of 5–7 mM, the surfactant recovery is observed to increase. This can be attributed to the decrease in the CMC of the surfactant caused by the lower pH, producing more surfactant micelles with a lower binding site. In turn, it facilitate the separation of the metal ions [48].

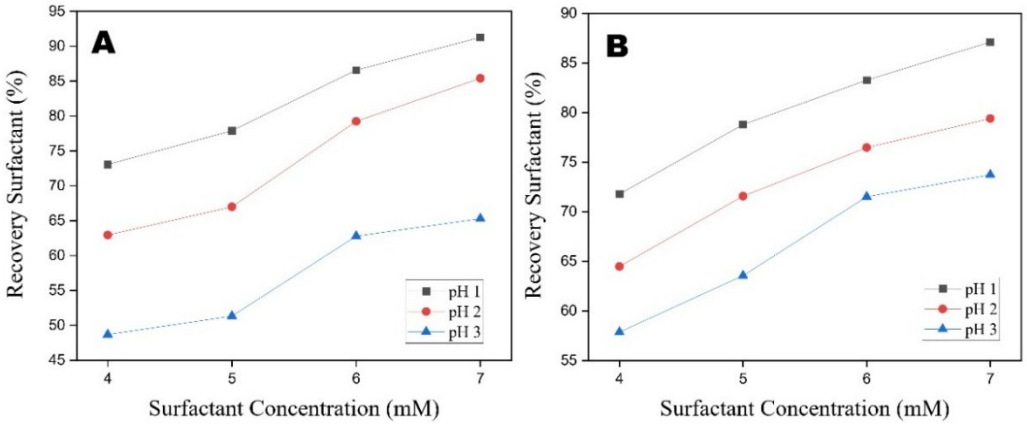

Fig. 3. Recovery of surfactants with metal ion Cu^{2+} (a) and Cd^{2+} (b)

Furthermore, Fig. 2 demonstrates that the CMC of the surfactant in a solution with a pH of 1 can decrease to 3 mM, representing a 62.5% reduction from the CMC of the pure surfactant. The decrease in CMC facilitates the formation of surfactant micelles. Thus, at a concentration of 6 mM, which is twice the CMC of the pure surfactant at pH 1, surfactant recovery can reach 87%. It has been observed that surfactant recovery decreases as surfactant concentration decreases and solution pH increases. The lowest recovery was observed at a surfactant concentration of 4 mM at pH 3, while the highest was at a concentration of 7 mM at pH 1.

The separation efficiency between metal ions and surfactant micelles was studied through metal ion rejection analysis. As depicted in Fig. 4, the amount of heavy metal ions successfully separated from the surfactant micelles, with the most separated metal ions achieved at pH 1, with a substantial decrease in separation observed at higher pH levels. In strongly acidic conditions, the abundant H^+ ions from the acid can compete with metal ions to replace the bonds between metal ions and surfactant micelles. The disruption of metal ion coordination was supported previously by the study showing that changing the pH influences the equilibrium and stability of metal-surfactant complexes of SDS-Cu(II) [49]. The metal ions released from the surfactant micelles then pass through the membrane during the ultrafiltration process. Meanwhile, the selectivity of metal ion rejection exhibited minimal differences between two different metal ions, Cu^{2+} and Cd^{2+}, with the highest rejection for Cu^{2+} at 59% and for Cd^{2+} at 55%. This percentage is the amount of metal ions released through the membrane, with some of the free metal ions remaining on the feed solution. For that reason, it is logical to conclude that the rejection rate is not perfect.

While the acid-assisted MEUF system exhibited moderate rejection rates for free metal ions, this approach provides several advantages compared to conventional recovery techniques such as precipitation or gel filtration. The recovery of used surfactant by precipitation and chelation methods requires the use of additional chemicals and a complex process [50]. While gel filtration is likely less efficient when employed on a large scale. On the other hand, acidification-UF is considered the simplest, cost-effective, and efficient process for surfactant recovery [47]. Despite having moderate rejection rates for free ions, eventually, the acidification-UF process has been shown to effectively separate the metal ions from the surfactant micelles while preserving the surfactant for the subsequent processes [51]. This process has a distinct advantage in comparison to other recovery methods.

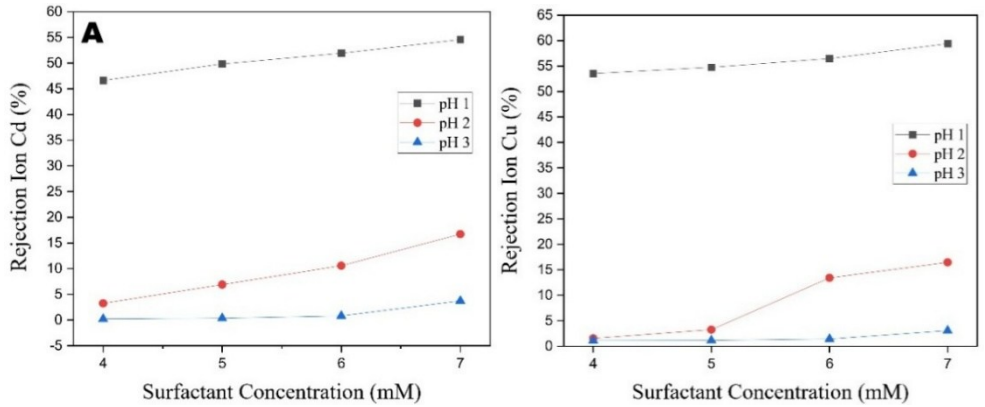

Fig. 4. Rejection of metal ion in variation of pH and surfactant concentration with metal ion Cu^{2+} (a) and Cd^{2+} (b)

The recovered surfactant was further evaluated to determine its effectiveness in capturing metal ions during the wastewater treatment process. The recovered surfactant was subjected to testing by the addition of 100 ppm of metal ions. As presented in Table 3, the amount of entrapped metal ions increases with the higher pH values during the recovery process. The performance of recovered surfactant in removing metal ions from the feed is satisfactory. In this study, 80.2% of Cu^{2+} ions and 81.1% of Cd^{2+} ions were removed from the feed, both at pH 3. The finding is consistent with the results of previous research, which demonstrated that at higher pH during the recovery process, the surfactant was still able to bind more than 50% of the metal ions. Another study utilized a chelating surfactant, C14-ED3A3Na, in MEUF which also demonstrated that the rates of metal ion removal increased as the pH value decreased, with optimal removal at a pH of 1 [52]. The previous study also demonstrated that the surfactant in a solution at a pH of 3 exhibited a superior capacity to bind metal ions in comparison to neutral pH at the same surfactant concentration [34]. This phenomenon is related to the electrostatic interaction between the SDS and the metal ions, which is more intense at low pH. This allows stronger binding of metal ions inside the surfactant micelles during MEUF [53].

Table 3. Metal ions removal using recovered surfactant

Metal ion	Removal Metal Ion (%)		
	pH 1	pH 2	pH 3
Cu^{2+}	48%	76%	80.20%
Cd^{2+}	53%	74%	81.10%

3.5. Flux profile and modeling of the membrane fouling mechanism

The results of the flux analysis are presented in Fig. 5, which demonstrated a continuous decreases in flux with increasing ultrafiltration time. The decline in flux during the ultrafiltration process can be divided into two stages. The first stage involves the formation of surfactant micelles, which then begin to adhere to the membrane surface and continue to accumulate. The second stage is characterized by the occurrence of stable state of adsorption of surfactant micelles on the membrane surface, which results in no significant further decrease in flux. This stage reflects the balance between the accumulation of surfactant micelles and diffusion [54].

As demonstrated in Fig. 5, the flux value is also influenced by the pH of the solution. At higher pH, the flux obtained is greater in comparison to that at lower pH levels. The reduction in flux at pH 1 can be attributed to micelle formation, as depicted in Table 2, where the surfactant micelles formed at this pH are larger compared to those at other pH levels. During the ultrafiltration process, micelles larger than the membrane pores are adsorbed onto the membrane, reducing the pore size and causing a significant decrease in flux [35]. In addition to the larger micelles at pH 1, the viscosity of the solution also increases as the pH decreases, which reduces the diffusivity of solutes and further reduces membrane flux [55].

In this study, the membrane fouling behavior was determined using the Hermia blocking model. The constant K for each model was calculated through nonlinear regression of the data presented in Fig. 5. According to the Hermia model, there are four membrane fouling mechanisms. The data was fitted to each of the four equation models, with the results presented in Fig. S-1. Furthermore, the parameter was calculated, and the result is presented in Table 4.

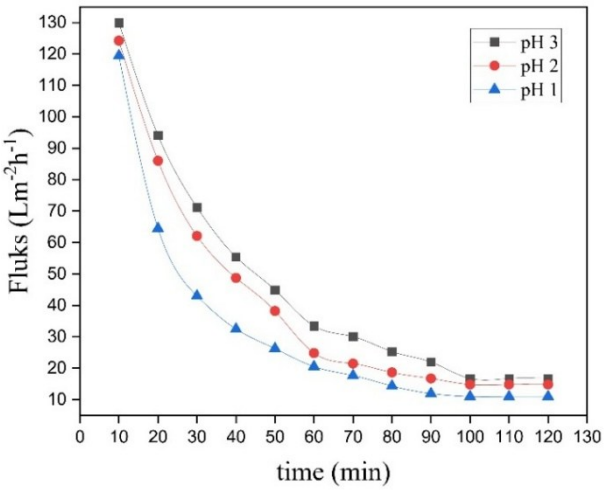

Fig. 5. Membrane flux with a surfactant concentration of 7 mM, metal ion concentration of 100 ppm, and varying solution pH

Table 4. Parameter of the fouling mechanism Hermia models

MEUF-conditions	Model	R2	K-Value
pH 3	Complete Blocking	0.9890	2.51×10^{-2}
	Internal Blocking	0.9989	1.59×10^{-3}
	Intermediate Blocking	0.8381	6.44×10^{-4}
	Cake Formation	-2.2015	1.00
pH 2	Complete Blocking	0.9881	2.92×10^{-2}
	Internal Blocking	0.9967	1.92×10^{-3}
	Intermediate Blocking	0.9113	7.03×10^{-4}
	Cake Formation	-1.7028	1.00
pH 1	Complete Blocking	0.9520	3.84×10^{-2}
	Internal Blocking	0.9936	2.78×10^{-3}
	Intermediate Blocking	0.9964	8.18×10^{-4}
	Cake Formation	-1.2117	1.00

As presented in Table 4, the R^2 value for model 2 at all pH variations is greater than 0.992, thus indicating that the membrane fouling mechanism at different pH levels is predominantly characterized by internal pore blocking. It has been demonstrated that the accumulation of the contaminants does not entirely cover the membrane's surface, rather, it is present between the membrane pores, indicating the internal pore blocking model. This phenomenon results in pore narrowing [31]. In the low pH condition, the functional groups on the PES protonated and the surface charge negativity reduced. This then affects the electrostatic interaction with anionic surfactants such as SDS, resulting on more hydrophobic surface [44]. The effect of this on the surface charge of the membrane, in combination with the hydrophobic interactions between the backbone of PES and the tails of SDS,

might be responsible for the intermediate blocking mechanism that has been observed. The existing literature also reports that the alteration of surface hydrophobicity and surface charge occur at low pH conditions [44]. This phenomenon is in coherence with the current observations of the SDS behavior at low pH. The lowest R^2 value is observed in model 4 (cake formation), making it unsuitable for describing the fouling mechanism in the ultrafiltration process in this study. The K value increases from pH 3 to pH 2, with the highest value at pH 1, indicating that the cake formed is thicker and correlates with the membrane flux. This phenomenon can be attributed to the formation of larger micelles, which enhance pore blocking.

The membrane surface morphology after the ultrafiltration process was analyzed by SEM, with the resultant data presented in Fig. 6. The Fig. demonstrates that fouling begins to form on the membrane surface at surfactant concentrations below the CMC value. At lower pH levels, fouling adheres more to cover the membrane pores [54]. This phenomenon is due to the fact that lower pH level results in the stimulation of fouling on the membrane, given that the surfactant concentration is lower than the pure surfactant CMC value [35].

SEM analysis also reveals the presence of a fouled membrane surface characterized by a rough and uneven surface. This is attributed to the accumulation of foulants, such as surfactant micelles and other contaminants, which also explains the reduction in flux over time during ultrafiltration processes. However, the SEM morphology reveals that the membrane pores are not fully clogged, which also confirms the result from the model calculation, indicating that the intermediate pore blocking mechanism is the most suitable model. Moreover, the SEM morphology of the membrane after the filtration process demonstrates that there is no disintegration of the membrane following filtration process with an acidic feed. This shows the stable performance of the PES membranes in this study under the short-term experimental acidic conditions (pH 1–3). Despite the absence of direct examination of the impact of long-term acid exposure in this work, the investigation of related phenomena remains a crucial avenue for further research. The previous literature reveals that the chemical integrity of PES membranes remains unchanged under acid conditions [56]. Nevertheless, to prevent the potential degradation of the membrane, it is possible to take into consideration the operation time and the feed pH during the application of acid-assisted MEUF [57].

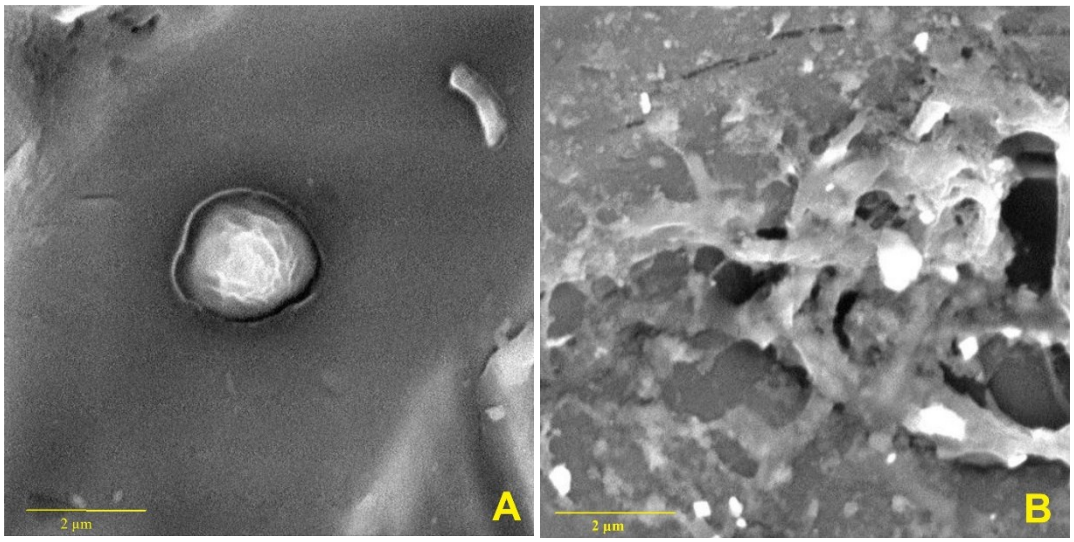

Fig. 6. SEM morphology of the new membrane (A), and the membrane after MEUF at pH 1 (B)

4. Conclusion

The findings of this research demonstrate that the acidification-MEUF process is an effective method for the removal of heavy metal ions, while simultaneously facilitating the recovery of surfactants. The findings indicate that pH 1 is the most effective for lowering CMC, with maximum surfactant recovery of 91% and 87.5% for Cu^{2+} and Cd^{2+} systems, respectively, at an initial surfactant concentration of 7 mM. The findings further demonstrate that the process of acidification has a direct impact on the CMC. The increase in pH has been shown to have direct correlation with a reduction of the amount of surfactant required to form micelles and remove metal ions. The spontaneous micelle formation process was confirmed thermodynamically with a negative value of ΔG_m at -44.95 - -40.56 kJ/mol. Furthermore, the recovered surfactant demonstrated the capacity to remove metal ions, exhibiting rejection rates of 91% for Cu^{2+} and 87% for Cd^{2+}. The modeling study revealed an internal pore blocking fouling mechanism at low pH conditions. These findings highlight the practical potential of acid-assisted MEUF for wastewater treatment with simultaneous surfactant recovery on a larger ultrafiltration scale.

Acknowledgements

This research was funded by the Annual Work Plan and Budget of Faculty of Engineering Universitas Diponegoro through the Scheme of Strategic Research "*Penelitian Strategis*" (Grant number: 89/UN7.F3/HK/V/2024).

References

1. M. Chen, N.P. Hankins, *Interaction among branched polyethylenimine (PEI), sodium dodecyl sulfate (SDS) and metal cations during copper recovery from water using polymer-surfactant aggregates*, J. Water Proc.

Eng. 34 (2020).
2. Z. Marzougui, M. Damak, B. Elleuch, A. Elaissari, *Occurrence and enhanced removal of heavy heavy metals wastewater treatment*, Adv. Sci. Technol. Innov. (2018) 535–538.
3. O.N. Kononova, G.L. Bryuzgina, O.V. Apchitaeva, Y.S. Kononov, *Ion exchange recovery of chromium (VI) and manganese (II) from aqueous solutions*, Arabian J. Chem. 12 (2019) 2713–2720.
4. N. Kaur, B. Juneja, S. Ballal, G.V.S. Prasad, A. Nanda, M. Kaur, F.M. Husain, H.S. Sohal, *Greener and efficient magnetic CS-Fe2O3 nanocomposite fabricated with β-Cyclodextrin for wastewater treatment: Heavy metal adsorption and photocatalytic degradation of industrial dyes,* J. Mol. Struct. (2025) 14310.
5. R. Mohadi, N.R. Palapa, T. Taher, P.M.S.B.N. Siregar, Normah, N. Juleanti, A. Wijaya, A. Lesbani, *Removal of Cr(VI) from aqueous solution by biochar derived from rice husk*, Commun. Sci. Technol. 6 (2021) 11–17.
6. L. Han, J. Li, Q. Xue, M. Guo, P. Wang, C. Sun, *Enzymatically induced phosphate precipitation (EIPP) for stabilization/solidification (S/S) treatment of heavy metal tailings*, Constr. Build. Mater. 314 (2022).
7. C. Goyburo-Ch´avez, J.I. Mendez-ruiz, S. Jim, P. Romero-crespo, L. Gutierrez, P.E. Valverde-armas, *Pilot-scale reverse osmosis treatment of gold cyanidation effluent for the removal of cyanide, heavy metal (loid)s, and ionic species*, Case Stud. Chem. Environ. Eng. 9 (2024) 100688.
8. N. Aryanti, A. Nafiunisa, A. Rizki, T. Djoko, *Synthesis, characterization and anti-fouling properties of poly[vinylidene fluoride]-incorporated SiO2, TiO2, ZrO2 nanoparticle-LiCl pore former ultrafiltration membranes*, Case Stud. Chem. Environ. Eng. 9 (2024) 100664.
9. N. Kusumawati, P. Setiarso, Supari Muslim, Sinta Anjas Cahyani, Nafisatus Zakiyah, A. Kahfi, *Effect of layered double hydroxide-graphene oxide modifier composition on characteristics of polyvinylidene fluoride based nanocomposite membranes in the separation of* Cu^{2+}, Commun. Sci. Technol. 9 (2024) 128–135.
10. N. Aryanti, A. Nafiunisa, V.F. Giraldi, L. Buchori, *Separation of organic compounds and metal ions by micellar-enhanced ultrafiltration using plant-based natural surfactant (saponin)*, Case Stud. Chem. Environ. Eng. 8 (2023) 2–11.
11. J. Ren, Y. Jiang, H. Ren, X. Xue, Z. Yang, L. Yang, *Micellar-enhanced ultrafiltration of heavy metal wastewater with palygorskite under various temperatures and pressures*, J. Water Process Eng. 67 (2024).
12. J. Huang, H. Li, G. Zeng, L. Shi, Y. Gu, Y. Shi, B. Tang, X. Li, *Removal of Cd(II) by MEUF-FF with anionic-nonionic mixture at low concentration*, Sep. Purif. Technol. 207 (2018) 199–205.
13. M. Dawam, M. Gobara, H. Oraby, M.Y. Zorainy, I.M. Nabil, *Advances in Membrane Technologies for Heavy Metal Removal from Polluted Water: A Comprehensive Review*, Water, Air, & Soil Pollut. 236 (2025) 1–20.
14. V. Innocenzi, M. Prisciandaro, F. Tortora, G. Mazziotti di Celso, F. Vegliò, *Treatment of WEEE industrial wastewaters: Removal of yttrium and zinc by means of micellar enhanced ultra filtration*, Waste Manag. 74 (2018) 393–403.
15. N. Abdullah, N. Yusof, W.J. Lau, J. Jaafar, A.F. Ismail, *Recent trends of heavy metal removal from water / wastewater by membrane technologies*, J. Ind. Eng. Chem. 76 (2019) 17–38.
16. F. Liang, L. Sun, Z. Zeng, J. Kang, *Treatment of surfactant wastewater by foam separation: Combining the RSM method and WOA-BP neural network to explore optimal process conditions*, Chem. Eng. Res. Des. 193 (2023) 85–98.
17. L.K.S. Tanwar, M.K. Banjare, S. Sharma, K.K. Ghosh, *Physicochemical studies on the micellization of anionic surfactants in the presence of long alkyl chain ionic liquid*, Chem. Phys. Lett. 769 (2021).
18. G. Simoni, X. Chen, M.L. Christensen, V. Boffa, *Treatment of printing industrial wastewater: application of acidification, coagulation and flocculation for dewatering*, J. Water Proc. Eng. 72 (2025).
19. L. Fu, G. Zhang, J. Ge, K. Liao, H. Pei, P. Jiang, X. Li, S*tudy on organic alkali-surfactant-polymer flooding for enhanced ordinary heavy oil recovery*, Colloids Surf. A Physicochem. Eng. Asp. 508 (2016) 230–239.
20. D. Kulkarni, N. Itankar, *Surfactant removal from wastewater: a comparative review on adsorption versus other techniques*, Environ. Technol. Rev. 14 (1) (2025) 713-742.
21. T. Najem, G.M. Ayoub, D. Salam, R.M. Zayyat, *Eliminating hazardous pollutants: treatment options for dioxins and surfactants from water and wastewater: an updated review*, Environ. Sci. Pollut. Res. 31 (2024) 62702–62729.
22. J. Huang, F. Qi, G. Zeng, L. Shi, X. Li, Y. Gu, Y. Shi, *Repeating recovery and reuse of SDS micelles from MEUF retentate containing Cd2+ by acidification UF*, Colloids Surf. A: Physicochem. Eng. Asp. 520 (2017) 361–368.
23. J. Huang, F. Yuan, G. Zeng, X. Li, Y. Gu, L. Shi, W. Liu, Y. Shi, *Influence of pH on heavy metal speciation and removal from wastewater using micellar-enhanced ultrafiltration*, Chemosphere 173 (2017) 199–206.
24. J. Huang, F. Qi, G. Zeng, L. Shi, X. Li, Y. Gu, Y. Shi, *Repeating recovery and reuse of SDS micelles from MEUF retentate containing Cd2+ by acidification UF*, Colloids Surf. A: Physicochem. Eng. Asp. 520 (2017) 361–368.
25. S.K. Rajendran, J.H. Mondal, Md.S. Alam, *Influence of an anionic hydrotrope on thermophysical properties of an anionic surfactant sodium dodecyl sulfate*, Chem. Phys. Lett. 787 (2022).
26. S. Shirzad, R. Sadeghi, *Micellization properties and related thermodynamic parameters of aqueous sodium dodecyl sulfate and sodium dodecyl sulfonate solutions in the presence of 1-propanol*, Fluid Phase Equilib. 377 (2014) 1–8.
27. J.A. Kozlova, D.A. Danilov, E. V Gordeev, *Determination of concentration of sodium dodecyl sulfate after intercalation of layered rare earth hydroxides determination of concentration of sodium dodecyl sulfate after intercalation of layered rare earth hydroxides*, the 2nd international conference on physical instrumentation and advanced materials, Surabaya, Indonesia, 050017 (2020).
28. Y. Zhai, J. Yang, *Fabrication and modification of PVDF membrane by PDA@ZnO for enhancing hydrophilic and antifouling property*, Arabian J. Chem. 16 (2023).
29. F. Tortora, V. Innocenzi, G. Mazziotti di Celso, F. Vegliò, M. Capocelli, V. Piemonte, M. Prisciandaro, *Application of micellar-enhanced ultrafiltration in the pre-treatment of seawater for boron removal*, Desalination 428 (2018) 21–28.
30. N. Park, H. Kim, Y. Lee, Y. Choi, S. Lee, *Prediction of ultrafiltration membrane fouling using statistical models in pilot and full-scale operations*, Desalin. Water Treat. 227 (2021) 86–92.
31. B. Niu, L. Yang, S. Meng, D. Liang, H. Liu, L. Yang, L. Shen, Q. Zhao, *Time-dependent analysis of polysaccharide fouling by Hermia models: Reveal the structure of fouling layer*, Sep. Purif. Technol. 302 (2022).
32. L.M.S. Silva, J.J. Galan-díaz, *Comparative analysis of critical micelle concentration of cationic surfactants determined by conductivity, sound velocity, and density using weighted orthogonal distance regression*, Surf. Interfaces 56 (2025).
33. A. Soria-Lopez, M. García-Martí, E. Barreiro, J.C. Mejuto, *Ionic surfactants critical micelle concentration prediction in water / organic solvent mixtures by arti fi cial neural network*, Tenside Surf. Det. 61 (2024) 519–529.
34. J.Y. Sum, W.X. Kok, T.S. Shalini, *The removal selectivity of heavy metal cations in micellar-enhanced ultrafiltration: A study based on critical micelle concentration*, Mater. Today Proc. 46 (2021) 2012–2016.

35. J. Huang, L. Shi, G. Zeng, H. Li, H. Huang, *Removal of Cd (II) by micellar enhanced ultra filtration: Role of SDS behaviors on membrane with low concentration*, J. Clean. Prod. 209 (2019).
36. M. Ishfaq, S. Mujeeb, A.M. Khan, *Surface activities and micellization of an anionic surfactant in the presence of a commercial insulin formulation*, J. Mol. Liq. 433 (2025).
37. M. Shakeel, K. Mehmood, M. Siddiq, *Solution and surface properties of metformin hydrochloride in aqueous solution and its interaction with amino acids and anionic surfactant, sodium dodecyl sulphate*, Proceedings of the National Academy of Sciences India Section A Physics and Science (2019).
38. K. Risse, J. Bridot, J. Yang, L. Sagis, S. Drusch, *Tuning interfacial properties of phospholipid stabilised oil – water interfaces by changing the phospholipid headgroup or fatty acyl chain*, J. Colloid Interface Sci. 686 (2025) 203–217.
39. Y. Sarkar, R. Majumder, S. Das, A. Ray, P.P. Parui, *Detection of curvature radius dependent interfacial pH/polarity for amphiphilic self-assemblies: positive vs negative curvature detection of curvature radius dependent interfacial ph/polarity for amphiphilic self-assemblies: positive versus negative curvature*, Langmuir 34 (21) (2017) 6271-6284.
40. B. Sarkar, *Micellar enhanced ultrafiltration in the treatment of dye wastewater: Fundamentals, state-of-the-art and future perspectives*, Groundw. Sustain. Dev. 17 (2022) 100730.
41] N. Farkas, J.A. Kramar, *Dynamic light scattering distributions by any means*, J. Nanoparticle Res. 23 (2021).
42. A.J. de Jesus Silva, M.M. Contreras, C.R. Nascimento, M.F. da Costa, *Kinetics of thermal degradation and lifetime study of poly(vinylidene fluoride) (PVDF) subjected to bioethanol fuel accelerated aging*, Heliyon 6 (2020).
43. B. Zhou, H. Yang, X. Li, Z. Li, S. Bauyrzhan, W. Kang, J. Shen, C. Ning, X. Yang, *A novel pH-responsive wormlike micelles combinated sodium dodecyl sulfate (SDS) and diethylenetriamine (DETA) based on noncovalent electrostatic interaction*, Phys. Fluids 35 (2023) 117110.
44. F. Matebese, M.L. Motloutsi, M.J. Raseala, R.M. Moutloali, *Smart ultrafiltration: pH-modulated polyacrylic acid-grafted polyethersulfone (PAA-g-PES) membranes for efficient natural organic matter (NOM) foul mitigation and cleaning process*, Chem. Eng. J. Adv. 24 (2025) 100935.
45. N.A. Volkov, N.V. Tuzov, A.K. Shchekin, *Molecular dynamics study of salt influence on transport and structural properties of SDS micellar solutions*, Fluid Ph. Equilib. 424 (2016) 114–121.
46. T. Mudalige, H. Qu, D. Van Haute, S.M. Ansar, A. Paredes, T. Ingle, *Chapter 11 - Characterization of nanomaterials: tools and challenges*, in: Nanomaterials for Food Applications, 2019: pp. 2019–2021.
47. A. Yusaf, M. Usman, M. Ibrahim, A. Mansha, A. ul Haq, H.F. Rehman, M. Ali, *Mixed micellar solubilization for procion blue MxR entrapment and optimization of necessary parameters for micellar enhanced ultrafiltration*, Chemosphere 313 (2023) 137320.
48. X. Mao, J. Cai, R. Wu, B. Liu, *Mechanisms and membrane fouling properties of dual surfactants coupling nanofiltration for multiple heavy metal rejection*, J. Clean. Prod. 501 (2025).
49. X. Peng, Z. Zhang, H. Chen, X. Zhang, X. Zhang, C. Tan, X. Bai, Y. Gong, H. Li, *The investigation of the binding ability between sodium dodecyl sulfate and Cu(II) in urban stormwater runoff*, J. Environ. Manag. 350 (2024) 119671.
50. Z. Peng, H. Chen, Y. Li, K. Feng, C. Wang, F. Liao, H. Deng, Y. Huang, *Chelating surfactant for the removal of heavy metals from wastewater and surfactant recovery,* Desalin. Water Treat. 206 (2020) 229–234.
51. F. Tortora, V. Innocenzi, I. De Michelis, F. Vegliò, G.M. Di Celso, M. Prisciandaro, *Recovery of anionic surfactant through acidification/ultrafiltration in a micellar-enhanced ultrafiltration process for cobalt removal*, Environ. Eng. Sci. 35 (2018) 493–500.
52. Z. Peng, H. Chen, Y. Li, K. Feng, C. Wang, *Chelating surfactant for the removal of heavy metals from wastewater and surfactant recovery*, Desalin. Water Treat. 206 (2020) 229–234.
53. M. Kosmulski, E. Ma, L. Ruchomski, *Two types of electrokinetic behavior of solid particles in the presence of anionic surfactants*, J. Colloid Interface Sci. 533 (2019) 34–41.
54. S.P. Verma, B. Sarkar, *Simultaneous removal of Cd (II) and p-cresol from wastewater by micellar-enhanced ultrafiltration using rhamnolipid: Flux decline, adsorption kinetics and isotherm studies*, J. Env. Manag. 213 (2018) 217–235.
55. A. Sinahroy, S.H. Kim, C.M. Chung, *Predicting membrane fouling in membrane bioreactor systems using viscosity: Impacts of environmental conditions and antifouling agents*, J. Env. Manag. 370 (2024) 122868.
56. C. Cabeza, A.E.G. Ahmed, M. Minauf, K. Wieland, M. Harasek, *Enhancing starch hydrolysate syrup purification: long-term ultrafiltration membrane performance under industrial conditions*, Sep. Purif. Technol. 382 (2026) 135998.
57. Y. Li, G. Zhao, G. Pan, H. Yu, G. Tang, F. Luo, T. Zhong, Y. Zhang, Y. Liu, *Thin-film composite nanofiltration membrane based on polysulfonamide for extremely acidic conditions*, Sep. Purif. Technol. 356 (2025) 129918.